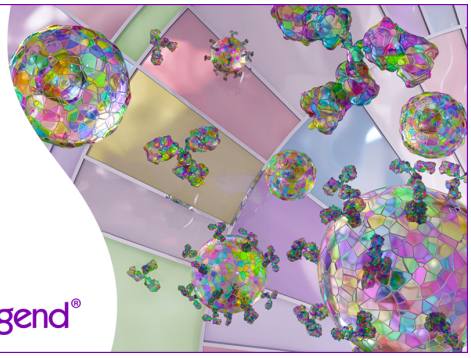

The Journal of Immunology
RESEARCH ARTICLE | MAY 15 2008

Antigen Sensitivity of CD22-Specific Chimeric TCR Is Modulated by Target Epitope Distance from the Cell Membrane[1] FREE

Scott E. James; ... et. al

J Immunol (2008) 180 (10): 7028–7038.
https://doi.org/10.4049/jimmunol.180.10.7028

Antigen Sensitivity of CD22-Specific Chimeric TCR Is Modulated by Target Epitope Distance from the Cell Membrane[1]

Scott E. James,*†‡ Philip D. Greenberg,*†‡ Michael C. Jensen,§ Yukang Lin,* Jinjuan Wang,* Brian G. Till,*† Andrew A. Raubitschek,§ Stephen J. Forman,§ and Oliver W. Press[2]*†

We have targeted CD22 as a novel tumor-associated Ag for recognition by human CTL genetically modified to express chimeric TCR (cTCR) recognizing this surface molecule. CD22-specific cTCR targeting different epitopes of the CD22 molecule promoted efficient lysis of target cells expressing high levels of CD22 with a maximum lytic potential that appeared to decrease as the distance of the target epitope from the target cell membrane increased. Targeting membrane-distal CD22 epitopes with cTCR$^+$ CTL revealed defects in both degranulation and lytic granule targeting. CD22-specific cTCR$^+$ CTL exhibited lower levels of maximum lysis and lower Ag sensitivity than CTL targeting CD20, which has a shorter extracellular domain than CD22. This diminished sensitivity was not a result of reduced avidity of Ag engagement, but instead reflected weaker signaling per triggered cTCR molecule when targeting membrane-distal epitopes of CD22. Both of these parameters were restored by targeting a ligand expressing the same epitope, but constructed as a truncated CD22 molecule to approximate the length of a TCR:peptide-MHC complex. The reduced sensitivity of CD22-specific cTCR$^+$ CTL for Ag-induced triggering of effector functions has potential therapeutic applications, because such cells selectively lysed B cell lymphoma lines expressing high levels of CD22, but demonstrated minimal activity against autologous normal B cells, which express lower levels of CD22. Thus, our results demonstrate that cTCR signal strength, and consequently Ag sensitivity, can be modulated by differential choice of target epitopes with respect to distance from the cell membrane, allowing discrimination between targets with disparate Ag density. *The Journal of Immunology,* **2008, 180: 7028–7038.**

We have previously demonstrated that human CD8$^+$ T cells can be modified by single-chain (fraction-variable) Ab (scFv)[3]-based chimeric TCR (cTCR) to promote redirected lysis of CD20$^+$ targets, and that such cells have potential efficacy for human tumor therapy (1–3). CD20 is expressed on a large majority of B cell malignancies (4, 5) and is a proven target for Ab-mediated immunotherapy (6–10), but these same features may also limit its utility as a tumor-associated Ag for recognition by cTCR$^+$ CTL. The anti-CD20 mAb rituximab is universally administered to patients with relapsed or refractory non-Hodgkin's lymphoma and persists in the serum at high concentrations for many months following cessation of treatment, which may interfere with Ag recognition by CD20-specific cTCR$^+$ CTL (8). Indeed, we previously showed that pretreatment of patient lymphoma samples with clinically significant concentrations of the anti-CD20 mAb 1F5 abrogates target lysis by CD20-specific cTCR$^+$ CTL in vitro (1). Additionally, normal B cells express high surface densities of CD20 (11), and although this can be overcome with Ab-mediated immunotherapy by administering saturating doses of the mAb, this large amount of self Ag may lead to deletion or anergy of adoptively transferred Ag-specific CTL (12).

To attempt to circumvent these limitations of targeting CD20 as a tumor-associated Ag, we have investigated CD22 as an alternative Ag for recognition by cTCR$^+$ CTL. CD22 is expressed on 60–70% of neoplastic B cells (13) and is detected at a lower copy number than CD20 on normal B cells (~30,000 CD22 vs 100,000–150,000 CD20 molecules/cell) (14, 15), which might limit the induction of anergy or deletion by normal B cells depending on the Ag sensitivity of the responding T cell. Additionally, because CD20 and CD22 are distinct Ags, the possibility exists for combined immunotherapies with anti-CD20 mAb and adoptive transfer of CD22-specific CTL, potentially yielding additive or synergistic activities against B cell malignancies.

When targeting CD22, however, the large extracellular domain of this molecule must be considered. Whereas CD20 is a tetraspanin-like protein with a small extracellular domain (16, 17), CD22 is comprised of seven Ig-like domains that provide a number of membrane-distal epitopes that can be recognized by distinct mAbs (18, 19). Recent work has revealed that activation of canonical TCR chains is critically dependent on the size of the MHC

*Fred Hutchinson Cancer Research Center, Seattle, WA 98109; †Division of Oncology, Department of Medicine, University of Washington, Seattle, WA 98195; ‡Department of Immunology, University of Washington, Seattle, WA 98195; and §City of Hope National Medical Center and Beckman Research Institute, Duarte, CA 91010

Received for publication January 2, 2008. Accepted for publication March 10, 2008.

The costs of publication of this article were defrayed in part by the payment of page charges. This article must therefore be hereby marked *advertisement* in accordance with 18 U.S.C. Section 1734 solely to indicate this fact.

[1] This research was supported by National Institutes of Health Grants R21 CA117131 (to O.W.P.), R01 CA76287 (to O.W.P.), CA18029 (to P.D.G.), and CA33084 (to P.D.G.); Lymphoma Research Foundation Grant MCLI-07-012; and gifts from Mary and Geary Britton-Simmons, David and Patricia Giuliani, the Hext Family Foundation, and James and Sherry Raisbeck (to O.W.P.). S.E.J. is supported by a stipend from the National Institutes of Health Medical Scientist Training Program, a Poncin Award, and an Academic Rewards for College Scientists Award.

[2] Address correspondence and reprint requests to Dr. Oliver W. Press, Fred Hutchinson Cancer Research Center, 1100 Fairview Avenue North, Seattle, WA 98109. E-mail address: press@u.washington.edu

[3] Abbreviations used in this paper: scFv, single-chain (fraction-variable) Ab; 7-AAD, 7-aminoactinomycin D; ABS, antibody binding sites; BLT, *N*-α-benzyloxycarbonyl-L-lysine thiobenzyl ester; cTCR, chimeric TCR; MFI, mean fluorescence intensity; PEG, polyethylene glycol; pMHC, peptide-MHC; WT, wild type.

ligand being recognized, with signaling attenuating sharply when the TCR:peptide-MHC (pMHC) ligand pair size exceeds wild-type dimensions (20). The mechanism underlying this phenomenon as proposed by the kinetic segregation model involves the inability of extended length T cell:target interaction sites to exclude the large extracellular domain-containing phosphatases CD45 and CD148 from the synaptic contact point, as normally occurs in the regions of tight T cell:APC membrane apposition generated by standard TCR:pMHC interactions (21). This loss of phosphatase exclusion can then lead to inefficient phosphorylation of the TCR complex and result in inefficient signaling (21). It has also recently been shown that chimeric immunoreceptors exhibit diminished signaling efficiency as the distance of the epitope from the target cell membrane increases, albeit to a lesser extent than seen with canonical TCR (22). These results suggest that the choice of epitope targeted on the CD22 molecule might influence signaling efficiency and potential therapeutic activity.

To better understand the impact on cTCR signaling of large cTCR:ligand pair sizes and to investigate targeting CD22 as a tumor-associated Ag for CTL-mediated immunotherapy, we generated two CD22-specific cTCR. One cTCR contains an engineered single-chain chimeric mAb (scFv) that binds to the first Ig-like domain of the CD22 molecule (far from the cell membrane), whereas the second cTCR was constructed with an scFv recognizing the third Ig-like domain, which is situated closer to the cell surface. Our findings demonstrate that the signal strength delivered by CD22-specific cTCR is modulated by the distance of the target epitope from the target cell membrane, with diminished Ag sensitivity observed when targeting membrane-distal epitopes. As a result of this phenomenon, CD22-specific cTCR$^+$ T cells are able to discriminate between targets expressing varying densities of CD22 when targeting this molecule at epitopes far from the target cell membrane: killing B cell lymphoma cell lines while demonstrating minimal lytic activity against normal B cells.

Materials and Methods

Antibodies

cTCR expression was analyzed with a PE-conjugated polyclonal goat anti-human Fcγ-specific IgG (Jackson ImmunoResearch Laboratories) or with a FITC-conjugated polyclonal goat anti-mouse F(ab′)$_2$-specific IgG (Sigma-Aldrich). CD20 and CD22 expression were analyzed with mouse anti-human mAbs (BD Pharmingen): PE anti-CD20 Quantibrite (clone L27), PE anti-CD22 (clone S-HCL-1), and PE-Cy5 anti-CD22 (clone HIB22). The RFB4-binding epitope of CD22 was detected with the PE-conjugated mouse anti-human CD22 mAb clone RFB4 (Chemicon International). cTCR were stimulated with polyclonal purified goat anti-human Fcγ-specific IgG (Jackson ImmunoResearch Laboratories).

Cell lines and primary cells

The Daudi, Raji, and Ramos B cell tumor cell lines and the Jurkat T cell line were obtained from American Type Culture Collection. The Phoenix G cell line was obtained from G. Nolan (Stanford University, Palo Alto, CA). Human PBMC were obtained from normal donors and positively selected for the CD8 or the CD19 Ags using immunomagnetic selection to obtain CD8$^+$ T cells and CD19$^+$ B cells, respectively (Miltenyi Biotec). The HD39 hybridoma line was a gift from E. Clark (University of Washington, Seattle, WA).

Molecular constructs

The CD20 and CD22 Ags were cloned by RT-PCR (One-step RT-PCR kit; Invitrogen) from total RNA obtained from PBMC (RNeasy; Qiagen). The Ig1-2 and Ig3-7;1-2 CD22-based ligands were generated by overlap extension PCR (PfuUltra; Stratagene). The cDNAs encoding the HD39 V_L and V_H Ig domains were obtained by RT-PCR amplification of total RNA obtained from the HD39 hybridoma cell line, as previously described (23, 24). The V_L and V_H Ig cDNA sequences were linked by overlap extension PCR with a DNA sequence encoding the peptide linker: GSTSGGGS GGGSGGGGSS. The RFB4 scFv template DNA was a gift from D. Fitzgerald (National Institutes of Health, Bethesda, MD). The HD39 and RFB4 scFv cDNAs were exchanged with the Leu16 scFv region of the Leu16 cTCR construct obtained from M. Jensen (City of Hope, Duarte, CA) using overlap extension PCR. The IFN-β scaffold attachment region was placed 3′ of the cTCR gene in reverse orientation, as previously described (25). Each DNA construct was cloned into the LZRS pBMN-z Moloney murine leukemia virus vector obtained from G. Nolan (Stanford University, Palo Alto, CA).

Retroviral transduction and cell culture

The Phoenix G packaging cell line was transfected with LZRS pBMN vectors containing genes of interest using Lipofectamine 2000 (Invitrogen). Stable transfectants were obtained following selection in 2 μg/ml puromycin (Invitrogen) and cultured in 175-cm^2 culture flasks (Corning Glass). Retroviral supernatants were obtained over 2 days and precipitated with polyethylene glycol (PEG; m.w. 8000; Sigma-Aldrich). A 5× PEG solution was added to retroviral supernatant for a final concentration 8 g/dL and allowed to precipitate for 24 h at 4°C, followed by centrifugation at 1500 × *g* for 1 h at 4°C. The pellets containing concentrated retrovirus were resuspended in 500 μl of RPMI 1640 each. A total of 3×10^6 Jurkat T cells was transduced by spin-fection with 1 ml of PEG-concentrated retroviral supernatant containing 4 μg/ml polybrene (Sigma-Aldrich) for 1 h at 32°C, 1500 rpm. The transduction cultures were then incubated at 37°C for 3 h, washed, and resuspended in culture medium. Jurkat T cell clones expressing varying densities of CD20 and CD22 were obtained by limiting dilution cloning following transduction. CD8$^+$ T cells were stimulated with 30 ng/ml OKT anti-CD3ε (Ortho Biotech) and 50 U/ml human rIL-2 (Chiron), and at 72 h, 3×10^6 CD8$^+$ T cells were transduced by the same procedure as for Jurkat T cells, with the addition of 50 U/ml human rIL-2. Primary human T cells were maintained by stimulation with irradiated PBMC, lymphoblastoid cell line, and anti-CD3ε every 14 days, as previously described (26). CTL expressing high densities of the cTCR were obtained by FACS sorting or by positive immunomagnetic selection using PE-conjugated polyclonal goat anti-human Fcγ-specific IgG, followed by anti-PE magnetic beads (Miltenyi Biotec). Miltenyi MS columns were used to enrich cells bound by anti-PE magnetic beads, according to the manufacturer's instructions.

CTL degranulation assay

A total of 2×10^5 T cells was stimulated by either plate-bound anti-Fcγ Abs (200 μg/ml) or 2×10^5 target cells (1:1 E:T ratio) in a volume of 200 μl of RPMI 1640 for 3–4 h at 37°C. Supernatants were obtained and analyzed using the *N*-α-benzyloxycarbonyl-L-lysine thiobenzyl ester (BLT) esterase assay, as previously described (27). Benzyloxycarbonyl-L-lysine thiobenzyl ester and 5,5′-dithiobis(2-nitrobenzoate) were purchased from Sigma-Aldrich. Briefly, 50 μl of culture supernatant was added to 100 μl of a solution of BLT and 5,5′-dithiobis(2-nitrobenzoate) at room temperature, and absorbance at 405 nm was measured at 30 min to determine the relative amount of esterase activity in the samples. Maximum release was determined by lysing T cells with 5 μl of 1% IGEPAL CA-630 (Sigma-Aldrich). Percentage of degranulation was determined by the following formula: % degranulation = $((A_{405,\ \text{sample}} - A_{405,\ \text{nonstimulated T cells}})/(A_{405,\ \text{lysed T cells}} - A_{405,\ \text{nonstimulated T cells}})) \times 100$.

Chromium release assay

Chromium release assays were performed, as previously described (1). Briefly, 2×10^3 ^{51}Cr-labeled targets were incubated with CTL in 200 μl of RPMI 1640 plus 10% FCS for 5 h, after which 30 μl of supernatant was assayed for the presence of radioactivity. Maximum release was determined by lysing target cells with 100 μl of 5% IGEPAL CA-630 (Sigma-Aldrich). The percentage of target lysis was calculated according to the following formula: % lysis = ((experimental ^{51}Cr release – spontaneous ^{51}Cr release)/(maximum ^{51}Cr release – spontaneous ^{51}Cr release)) × 100.

cTCR and Ag quantitation

The number of CD20 and CD22 molecules expressed by Jurkat clones, tumor cell lines, and autologous B cells was estimated as Ab binding sites (ABS) using Quantibrite beads (BD Pharmingen), the PE-labeled anti-CD20 mAb L27, and the PE-labeled anti-CD22 mAb H-SCL-1 (BD Pharmingen) with known fluorescence to protein ratios at saturating concentrations, according to the manufacturer's instructions. The number of cTCR expressed by CD8$^+$ T cells was estimated using FITC-conjugated Quantum microbeads (Bangs Laboratories) and saturating concentrations of FITC-conjugated polyclonal goat anti-mouse F(ab′)$_2$-specific IgG (Sigma-Aldrich) with known fluorescence to protein ratio.

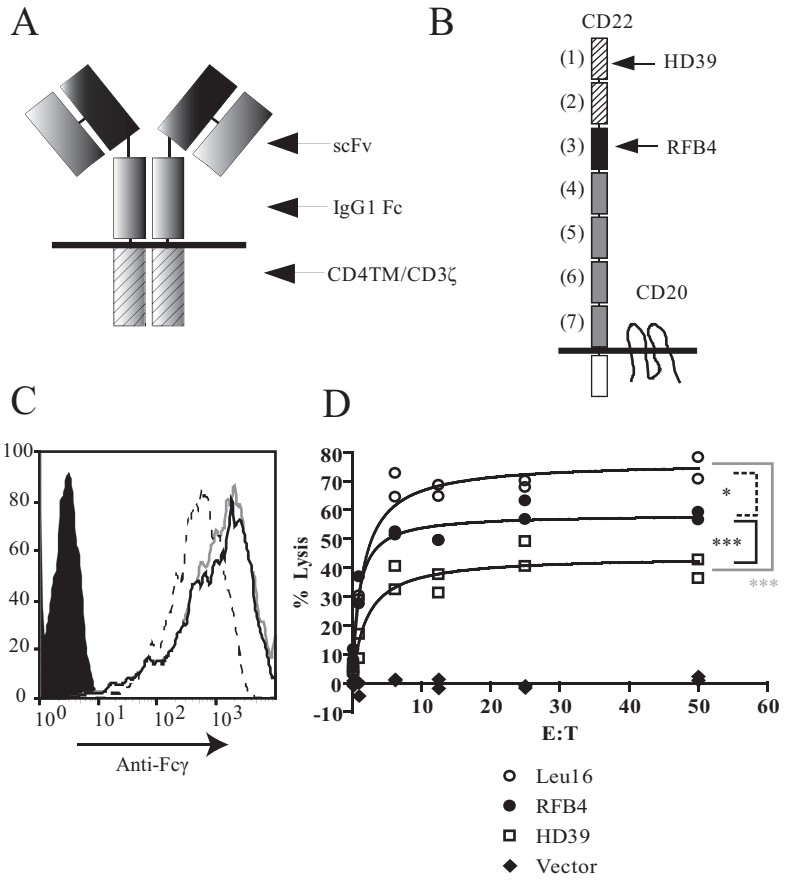

FIGURE 1. Maximum lytic efficiency of cTCR$^+$ CTL correlates with the distance of the target Ag epitope from target cell membrane. *A*, Schematic of cTCR structure. IgG1 Fc, C_H1 hinge and C_H2 and C_H3 domains of IgG1; CD4TM, CD4 transmembrane. *B*, Epitope mapping of HD39 and RFB4 scFv binding sites of CD22. CD20 is shown to scale. *C*, Flow cytometric measurement of cTCR expression. cTCR or vector-transduced CTL were stained with PE-labeled goat anti-human Fcγ-specific polyclonal IgG. Black solid, empty vector; black line, Leu16; gray line, RFB4; and dashed line, HD39. *D*, Target lysis assay using ^{51}Cr-labeled CD20$^+$CD22$^+$ Daudi cell line as targets. The data are representative of four experiments. Points represent individual samples. *, $p < 0.05$; ***, $p < 0.0001$: paired *t* test, two tailed. Dashed line, Leu16 vs RFB4 (*); solid black line, RFB4 vs HD39 (***); gray solid line, Leu16 vs HD39 (***).

Flow cytometric target lysis assay (7-aminoactinomycin D (7-AAD) assay)

CTL were labeled with 10 μM DDAO succinimidyl ester (Molecular Probes), and target cells were labeled with 1 μM CFSE (Molecular Probes) and incubated at a 30:1 E:T ratio (3×10^5 T cells; 1×10^4 target cells) in a 96-well plate for 4 h at 37°C. The cells were then resuspended in 7-AAD (Molecular Probes) at 2 μg/ml, and CSFE$^+$ DDAO$^-$ 7-AAD$^+$ dead target cells were enumerated by flow cytometry. The proportion of each dead target cell in the absence of T cells was subtracted from each sample value to obtain specific lysis values. CTL were regularly used on days 12–14 of 14-day restimulation cycles.

cTCR down-modulation assay

CTL were labeled with 10 μM DDAO succinimidyl ester (Molecular Probes), and target cells were labeled with 1 μM CFSE (Molecular Probes) and incubated at a 1:1 E:T ratio (2×10^5 T cells; 2×10^5 target cells) in a 96-well plate for 4 h at 37°C. The cells were then resuspended in a saturating concentration of PE-conjugated polyclonal goat anti-human Fcγ-specific IgG (anti-cTCR), and the mean fluorescence intensity (MFI) of cTCR staining on DDAO$^+$ CFSE$^-$ T cells was determined by flow cytometry. Percentage of cTCR down-modulation was calculated by the following formula: % cTCR down-modulation = 100 × (1 − stimulated MFI/unstimulated MFI).

Statistical analysis

Chromium release curves of cTCR$^+$ CTL in response to Daudi lymphoma line cells were compared using a two-tailed, paired *t* test using GraphPad Prism software.

Results

The maximum lytic efficiency of cTCR$^+$ CTL correlates with the distance of the target Ag epitope from target cell membrane

We generated two CD22-specific cTCR based on our previously described CD20-specific cTCR (denoted Leu16), consisting of a scFv Ag recognition module, an IgG1 Fc spacer promoting dimerization, the CD4 transmembrane domain, and the CD3ζ cytoplasmic domain as the signal transducer (Fig. 1*A*). The scFv sequences for these cTCR were derived from the CD22-specific mAbs RFB4 and HD39, which by epitope mapping bind to the third and first Ig-like domains of CD22, respectively (18, 28) (data not shown; Fig. 1*B*). Thus, the HD39 cTCR:CD22 ligand pair is expected to result in the largest distance between the T cell and target, followed by the intermediate-sized RFB4 cTCR:CD22 ligand pair, and finally the relatively small Leu16 cTCR:CD20 ligand pair recognizing the short tetraspanin-like CD20 molecule.

The three cTCR constructs were transduced with a retroviral vector into human CD8$^+$ T cells, and the resulting cell lines were selected for similar cTCR expression by fluorescence-activated cell sorting (Fig. 1*C*). These cell lines were then tested for lytic activity against the CD20$^+$CD22$^+$ B cell lymphoma line Daudi in a standard chromium release assay. The lytic activity of transduced CTL lines correlated with the size of the cTCR:ligand pair, with the Leu16 CD20-specific cTCR$^+$ CTL line producing the highest maximal level of target lysis (~75%), followed by the RBF4 (~60%) and HD39 (~40%) CD22-specific cTCR$^+$ CTL lines (Fig. 1*D*). This descending hierarchy of lysis was reproducible in four independent experiments, suggesting that the diminished lytic efficiency of the CD22-specific lines might result from the relatively large distances of their target Ag epitopes from the target cell membranes.

The diminished cytotoxicity of CD22-specific cTCR$^+$ CTL is not due to insufficient target Ag density, insufficient cTCR expression density, or low affinity of scFv

Although the differential target lysis induced by the three cTCR correlated with cTCR:ligand pair size, these differences could reflect other factors such as target Ag density or cTCR scFv affinity. To assess these possibilities, we compared the Ag sensitivity of

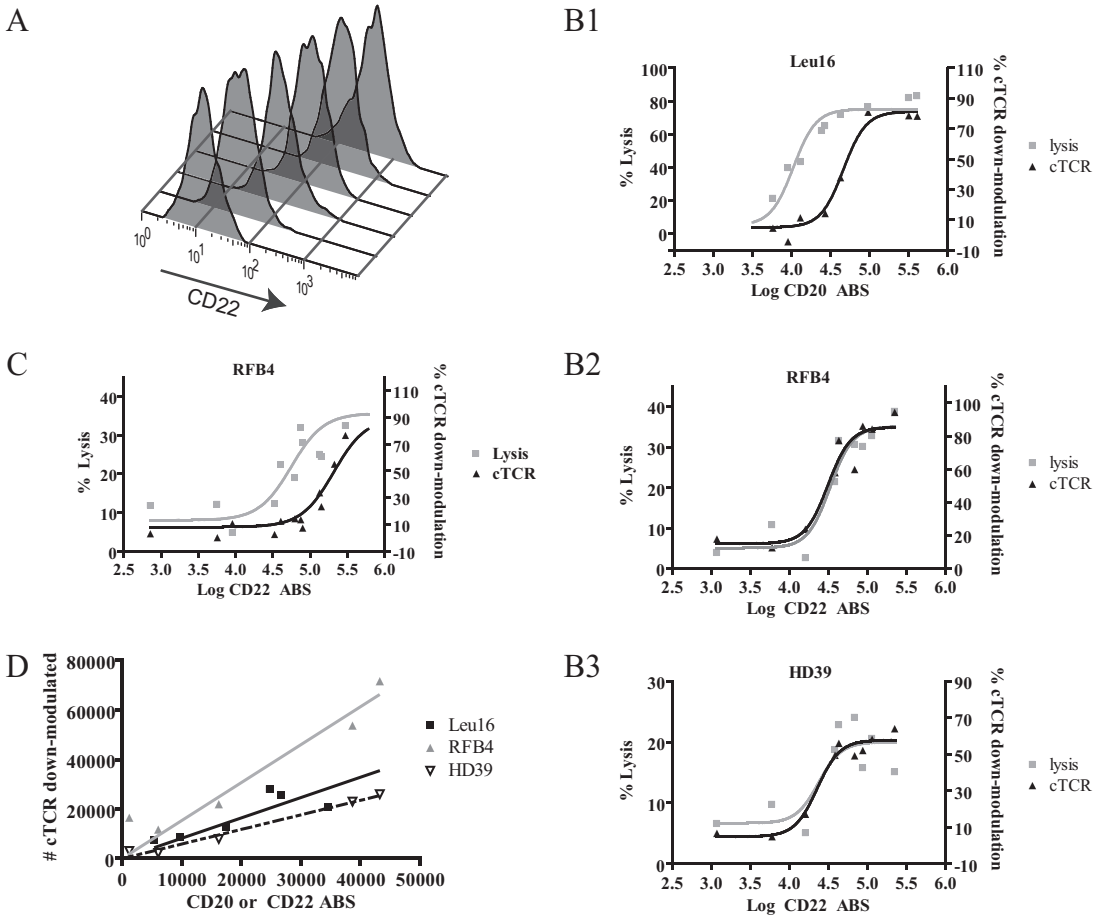

FIGURE 2. Lysis defect of CD22-specific cTCR is not due to insufficient target Ag density, insufficient cTCR expression density, or low affinity of scFv. *A*, Flow cytometry of transduced CD22$^+$ Jurkat clones with varying surface density. Cells were stained with PE-H-SCL-1 anti-CD22 mAb. Six clones of 12–15 total per Ag type are shown. Similar results were obtained for CD20$^+$ Jurkat clones. *B*1, *B*2, *B*3, and *C*, Ag sensitivity of target lysis and cTCR down-modulation. The 7-AAD lysis assay and cTCR down-modulation assay were performed, as described in *Materials and Methods*. The expression density of the RFB4 cTCR is 5-fold greater on the CTL line used in *C* compared with the RFB4 cTCR$^+$ CTL used in *B.2*. Points represent the average of duplicate samples in this and all following dose-response experiments. *D*, Relationship between Ag density and cTCR down-modulation. Numbers of cTCR expressed per T cell were estimated, as described in *Materials and Methods*. Data from cTCR down-modulation assay were converted from percentages to absolute numbers of down-modulated cTCR. Numbers of cTCR down-modulated were plotted vs numbers of CD20 or CD22 ABS (estimated as described in *Materials and Methods*) for Ag densities below the cTCR down-modulation inflection point. Data are representative of at least three experiments.

target lysis induced by the three cTCR expressed at similar copy number (~10^5 cTCR/cell) in response to Jurkat clones expressing varying densities of CD20 and CD22 (Fig. 2*A*). The numbers of CD20 or CD22 ABS per Jurkat target cell clone were estimated using saturating concentrations of PE-labeled mAbs with known fluorescence to protein ratios, with the observed median fluorescence intensities compared with a standard curve constructed using microbeads possessing known numbers of conjugated PE molecules. The Leu16 CD20-specific cTCR$^+$ CTL demonstrated half-maximal lysis (EC_{50}) at ~15,000 ABS/cell, whereas the CD22-specific cTCR$^+$ CTL demonstrated a lytic EC_{50} of ~50,000 ABS/cell (Fig. 2, *B.1* vs *B.2* and *B.3*). The CTL expressing the different cTCR exhibited differential maximum target lysis of the Jurkat clones with Leu16 ~75%, RFB4 ~35%, and HD39 ~20% (Fig. 2, *B.1*, *B.2*, and *B.3*, respectively). Thus, although the CD20-specific cTCR demonstrated a 3-fold higher Ag sensitivity than the CD22-specific cTCR based on requirement for ABS/cell, a descending hierarchy of lytic potential remained evident at saturating Ag densities. This suggested that differential Ag sensitivity of the cTCR or insufficient Ag expression by target cell lines did not account for the differences in the maximum lytic efficiencies observed among the three cTCR.

One potential explanation for the reduced lytic activity of the cells targeting CD22 is that the CD22-specific cTCR were expressed at insufficient copy numbers to promote lysis as efficiently as the CD20-specific cTCR. This could occur if the avidity of target Ag recognition by the CD22-specific cTCR was lower than that of the CD20-specific cTCR, requiring a greater cTCR expression density to induce maximal cTCR:Ag interaction and signaling according to the law of mass action as previously noted for canonical TCR (29, 30). Previous work has demonstrated that down-modulation of canonical TCR in response to strong pMHC agonists can be correlated with the sensitivity of Ag recognition and effector functions (31, 32). Furthermore, it has been demonstrated that low TCR expression density results in triggering too few receptors to promote maximal effector function (32). CD3ζ-based chimeric receptors have been shown to down-modulate similarly when triggered, suggesting cTCR down-modulation could also be used as a measure of T cell activation and Ag recognition sensitivity (33, 34). We therefore analyzed Ag-induced cTCR down-modulation to compare the relative avidity of Ag recognition among the three cTCR$^+$ CTL lines, selected for expression of similar numbers of cTCR (~10^5 cTCR/cell). Similar to target lysis, cTCR down-modulation followed a sigmoid relationship with

respect to Ag density for all three lines, with half-maximal cTCR down-modulation occurring at very similar Ag densities (Fig. 2*B*). This suggested that the functional avidity of Ag recognition was similar among the three cTCR. At $\sim 10^5$ cTCR/cell, the target cell Ag density required for half-maximal target lysis induced by the Leu16 cTCR was lower than that required for half-maximal cTCR down-modulation, suggesting that maximum lysis induction required only a portion of the cTCR population to be triggered and down-modulated, similar to findings with canonical TCR (35). In contrast, the CD22-specific cTCR demonstrated overlapping target lysis and cTCR down-modulation curves, suggesting that activation of all of the cTCR expressed by these CTL was required to induce the observed level of target lysis. These results implied that the CD22-specific cTCR were promoting lysis less efficiently than the Leu16 cTCR despite recognizing Ag and down-modulating similarly at similar target Ag densities. Therefore, CD22-specific cTCR expression density might be limiting maximal lysis, possibly due to diminished lysis per triggered TCR rather than insufficient cTCR affinity.

To test the hypothesis that insufficient cTCR expression density was limiting the maximum lysis induced by CD22-specific cTCR at saturating Ag densities, an RFB4 cTCR$^+$ CTL line was generated that expressed 5-fold greater numbers of the cTCR ($\sim 5 \times 10^5$ cTCR/cell) than the RFB4$^+$ CTL lines used in previous experiments by sorting the transduced CTL shortly after transduction using an immunomagnetic selection method. Furthermore, we performed the analysis earlier in the restimulation cycle (day 7–9), when the long terminal repeat-driven cTCR expression was higher than at later time points in the restimulation cycle when the previous experiments were performed (day 12–14; data not shown). The RFB4 cTCR$^+$ CTL line expressing greater numbers of cTCR required more Ag molecules expressed per target cell to induce half-maximal cTCR down-modulation; however, neither the Ag sensitivity nor the maximum efficiency of target lysis increased (Fig. 2, *B.2* vs *C*). This finding suggests that cTCR expression density was not limiting the diminished lytic Ag sensitivity or maximum efficiency of the RBF4 cTCR because maximal target lysis occurred at a lower Ag density than was necessary to down-modulate all the cTCR.

We noted that the sigmoid relationship between Ag density and cTCR down-modulation can be approximated by an exponential relationship at values below the inflection point on a logarithmic axis (data not shown). When plotting the number of cTCR down-modulated vs Ag density on a linear axis, the relationship is linear and close to 1:1 for all three cTCR below the inflection point, i.e., where availability of cTCR is not limiting (cTCR down-modulated:Ag ratios: Leu16 = 0.61 ± 0.20, RFB4 = 1.1 ± 0.33, HD39 = 0.45 ± 0.13, average of three experiments) (Fig. 2*D*). This linearity has been noted by Viola and Lanzavecchia (32) when triggering canonical TCR with high-affinity anti-CD3 mAb, but contrasts with the logarithmic relationship between pMHC ligand density and $\alpha\beta$ TCR triggering, which reflects the phenomenon of serial triggering in this setting (with a single pMHC triggering as many as 200 TCR) (36). This implies that the observed impaired maximum lytic potential of the CD22-specific cTCR does not derive from insufficient Ag-binding efficiency because all three cTCR recognize Ag and down-modulate with similar sensitivity. These results also suggest that cTCR do not serially engage Ag molecules, potentially accounting for relatively low extent of cTCR down-modulation and target lysis observed in response to targets expressing fewer than 10^4 Ag equivalents.

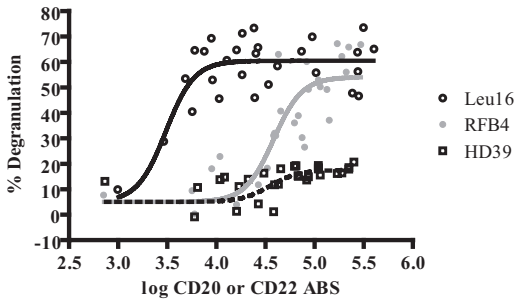

FIGURE 3. Targeting membrane-distal epitopes produces both a degranulation and granule-targeting defect. Degranulation of cTCR$^+$ CTL in response to Jurkat clones expressing varying densities of CD20 or CD22. Degranulation was assessed by BLT esterase activity, as described in *Materials and Methods*. Data from three experiments are overlaid.

Targeting membrane-distal epitopes produces both a degranulation and granule-targeting defect

The previous results suggested that a signaling defect might result from the relatively large cTCR:ligand pair sizes of the CD22-specific cTCR. It remained possible, however, that targeting membrane-distal epitopes could impair efficient targeting of lytic granules onto target cells, resulting in diminished lysis. We therefore analyzed the Ag sensitivity and efficiency of cTCR-induced degranulation in response to CD20 and CD22. The Leu16 CD20-specific cTCR induced maximal degranulation at relatively low Ag density (Fig. 3). In contrast, the HD39 CD22-specific cTCR induced very limited degranulation evident only at high Ag densities, suggesting a signaling defect from this cTCR. An intermediate phenotype was observed with the RFB4 CD22-specific cTCR: the maximum degranulation achieved was similar to that observed with the Leu16 CD20-specific cTCR (RFB4 = 54%, Leu16 = 60%, average of three experiments), but the sensitivity was much lower, requiring an Ag density for half-maximal degranulation similar to that observed for the HD39 cTCR (Fig. 3). Thus, despite promoting degranulation nearly equivalently to the Leu16 cTCR at saturating Ag densities, the RFB4 cTCR promoted lysis much less efficiently (Leu16 = 71% vs RFB4 = 39%, averaged over three or more experiments; Fig. 2, *B.1* vs *B.2*). These data suggest targeting membrane-distal epitopes results in both a degranulation and a granule-targeting defect.

Targeting membrane-distal epitopes results in diminished signaling per triggered cTCR

The preceding data suggested that whereas the three cTCR recognize Ag and down-modulate with similar avidity, the strength of the signal produced by the Leu16 CD20-specific cTCR is greater than that generated by the CD22-specific cTCR responding to wild-type (WT) CD22. Plotting the percentage of degranulation vs the number of cTCR down-modulated revealed that both the Leu16 CD20-specific cTCR and RFB4 CD22-specific cTCR responded similarly after the threshold for activation was reached, but that the signaling efficiency of the Leu16 cTCR was 10-fold greater per cTCR than the RFB4 cTCR (Fig. 4*A*). These data suggest that $\sim 10^4$ Leu16 cTCR must be triggered to achieve maximum degranulation, a value similar to that reported to be required for maximum production of IFN-γ by CTL responding via the endogenous TCR chains to pMHC (32). In contrast, triggering of far more RFB4 cTCR was required to produce the same level of degranulation ($\sim 10^5$ cTCR, average of four experiments). Similar values were observed for target lysis (Fig. 4*B*). Because the HD39 cTCR was only partially down-modulated in response to WT

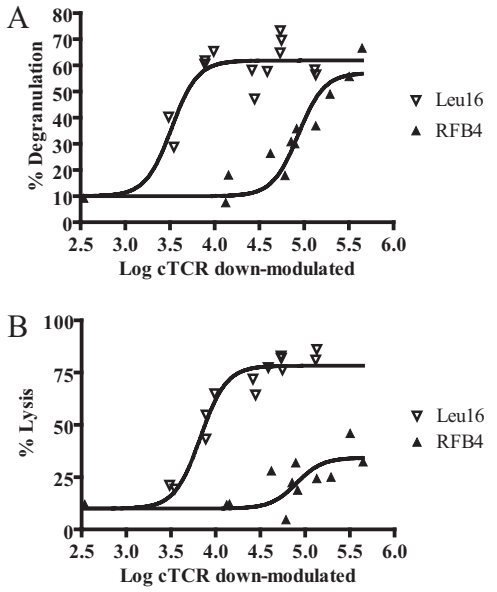

FIGURE 4. Targeting membrane distal epitopes results in diminished signaling per triggered cTCR. cTCR down-modulation was determined in simultaneous experiments in which target lysis and degranulation were also measured. The number of cTCR expressed per CTL was estimated, as described in *Materials and Methods*, and converted to the number of cTCR down-modulated. Percentage of degranulation (*A*) or percentage of target lysis (*B*) in response to a particular Ag density was plotted against the number of cTCR down-modulated in response to the same Ag density. One representative experiment of three is shown.

CD22 (Fig. 2*B.3* and data not shown), we could not directly compare the relationship between degranulation and the number of cTCR down-modulated with the values obtained for the Leu16 and RFB4 cTCR. Thus, whereas the RFB4 cTCR could be down-modulated similarly and at high Ag density promoted degranulation equivalently to the Leu16 cTCR, the strength of signal delivered per cTCR appeared to be far weaker.

Targeting a truncated CD22-based ligand restores sensitivity and efficiency of degranulation and target lysis

We next investigated the role of ligand size on the Ag sensitivity and efficiency of lysis and degranulation promoted by CD22-specific cTCR. Activation of TCR by immobilized Abs has been shown to exclude the large extracellular domain-containing phosphatase CD148 from the T cell contact site, which is essential for efficient signaling. In contrast, soluble anti-TCR Abs failed to promote exclusion, contributing to inefficient signaling (37). We first tested degranulation in response to stimulation of the RFB4 and HD39 cTCR with plate-bound Fcγ-specific polyclonal goat anti-human Abs. Unlike what was observed with recognition of targets expressing CD22, the maximum values of degranulation achieved with the RFB4 and HD39 cTCR were similar, demonstrating that the HD39 cTCR could promote efficient signaling if properly triggered (Fig. 5*A*). To determine whether the signaling defect observed following Ag recognition by the HD39 cTCR could be corrected if it was recognizing a smaller ligand, we next generated a truncated CD22 molecule in which the five membrane-proximal Ig-like domains were deleted and the molecule contained only the first two Ig-like domains and the full transmembrane and intracellular sequences of CD22 (Fig. 5*B*). This molecule, denoted Ig1-2, contains the HD39 epitope in the first Ig-like domain, but lacks the RFB4 epitope in the third Ig-like domain of CD22. Jurkat T cells were transduced with either WT CD22 or Ig1-2, and unsorted populations expressing similar intermediate levels of each ligand were used to test RFB4 and HD39 cTCR$^+$ CTL lines for degranulation. As expected, the RFB4 cTCR was unable to respond to the Ig1-2 molecule, but induced degranulation in response to WT CD22. In contrast, the HD39 cTCR induced degranulation in response to the Ig1-2 molecule to an extent similar to that observed with RFB4 cTCR responding to WT CD22, but again induced little degranulation in response to full-length CD22 (Fig. 5*C*). To determine whether targeting the truncated ligand improved the Ag sensitivity of degranulation compared with that observed when targeting WT CD22, we generated a panel of Jurkat T cell clones with varying expression densities of Ig1-2, as previously performed with CD20 and CD22 WT molecules. The HD39 cTCR$^+$ CTL line degranulated to a much greater extent in response to the Ig1-2$^+$ Jurkat clones compared with its response to the WT CD22$^+$ clones, consistent with the hypothesis that ligand size modulates the sensitivity of signaling leading to degranulation (Fig. 5*D*). Target lysis was also enhanced, suggesting that reducing the ligand size also rescued the granule-targeting defect observed when targeting membrane-distal epitopes of CD22. We found that the lytic Ag sensitivity and maximum lysis observed for the HD39 cTCR$^+$ CTL line targeting Ig1-2 and the Leu16 cTCR$^+$ CTL line targeting CD20 were very similar, suggesting that cTCR:ligand pair size and not an HD39 cTCR-intrinsic defect or the nature of the epitope being targeted was responsible for diminished signaling seen in response to WT CD22 (Fig. 5*E*). These data suggest that targeting membrane-distal epitopes diminishes the signal strength produced by cTCR, thereby diminishing the sensitivity of Ag recognition.

Membrane-distal target epitopes are not inhibitory in the presence of membrane-proximal ones

Previous experiments using artificially elongated mutants of the adhesion molecule CD48 expressed on target cells demonstrated that increasing the CD48:CD2 ligand pair size inhibited interactions of the much smaller TCR:pMHC ligand pair, as evidenced by diminished TCR down-modulation and IL-2 production by T cells (38). This finding suggested that the artificially enlarged mutant CD48:CD2 ligand pair might inhibit TCR signaling by generating an enlarged effector:target intermembrane space, interfering with the coaptation of the smaller cTCR:ligand pairs. A similar phenomenon of signal inhibition has been observed with T cells targeting artificially elongated pMHC molecules. This inhibition was found to correlate with an increased intercellular distance between target and effector cell membrane (20). The signal inhibition in this setting is proposed by the kinetic segregation model to arise from lack of exclusion of large extracellular domain-containing phosphatases from TCR microclusters as a result of this increased intermembrane distance, which could result in diminished TCR phosphorylation and signal strength (21). Thus, previous work has suggested that close apposition of target and effector cell membranes is necessary to ensure robust signaling during Ag recognition. Consequently, simultaneously targeting small ligands in the presence of large ones might inhibit efficient signaling by preventing this close interaction.

CD22, like many other proteins, is expressed as long and short isoforms, which for CD22 differ by two Ig-like domains. The smaller isoform, however, represents less than 1% of total cellular CD22, suggesting that responses to the larger isoform will predominate (39). Because the HD39 cTCR responded weakly to the large WT CD22 molecule and strongly to the truncated Ig1-2 molecule, we wished to model how a CTL expressing a cTCR would function if it encountered a target cell concurrently expressing a large and small isoform of the same protein. We selected a Jurkat clone demonstrating very high

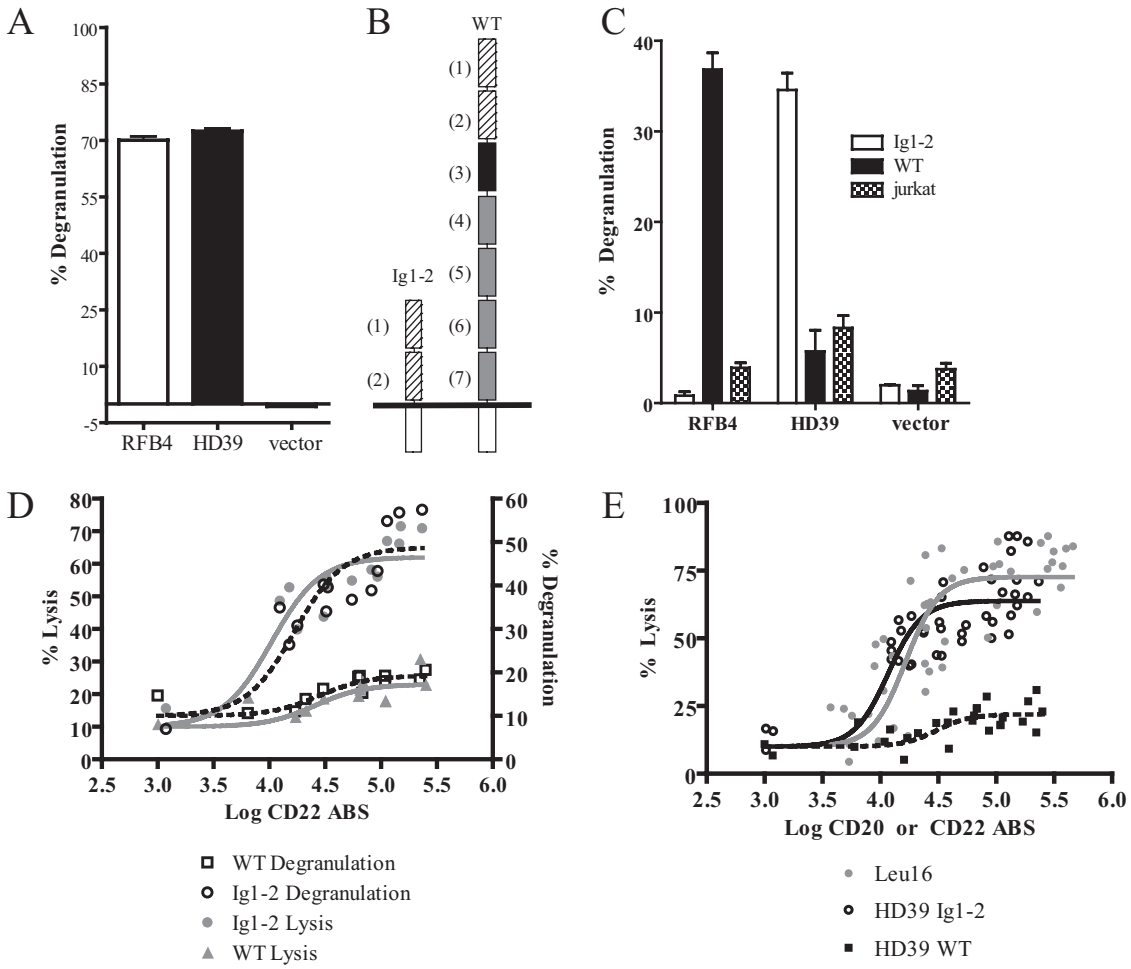

FIGURE 5. Targeting a truncated CD22-based ligand restores sensitivity and efficiency of degranulation and target lysis. *A*, RFB4 or HD39 cTCR$^+$ or empty vector-transduced CTL were incubated on goat anti-human Fcγ-specific IgG-coated plates (200 μg/ml) for 2 h in 100 μl of RPMI 1640. Supernatants were obtained and degranulation was determined in a BLT esterase assay. Average and SD of duplicate samples are shown and are representative results from one of three experiments. *B*, Schematic of truncated CD22-based ligand Ig1-2. *C*, Degranulation in response to unsorted transduced Jurkat cells expressing similar, intermediate densities of WT CD22 or Ig1-2. Average and SD of duplicate samples are shown and are representative of two experiments. *D*, Degranulation (BLT assay) or target lysis (7-AAD assay) by HD39 cTCR$^+$ CTL in response to Jurkat clones expressing varying densities of WT CD22 or Ig1-2. Representative results from one of three experiments are shown. *E*, Overlay of data from three experiments in which target lysis by Leu16 or HD39 cTCR$^+$ CTL was analyzed in response to Jurkat clones expressing varying Ag densities of CD20 or CD22 WT and Ig1-2, respectively.

expression of the Ig1-2-truncated CD22 molecule, transduced it with WT CD22, and sorted for expression of the RFB4 epitope at very high intensity to obtain a Jurkat line that was simultaneously WT CD22^{high} and Ig1-2^{high}. This cell line, denoted WT:Ig1-2, was lysed by the RFB4 cTCR$^+$ CTL line as efficiently as in previous experiments using CD22 WT^{high} Jurkat clones (Fig. 6*A* vs Fig. 2, *B.2* and *C*, and Fig. 4*B*), affirming high functional expression of the full-length WT CD22 molecule. The HD39 cTCR$^+$ CTL line lysed both the WT:Ig1-2 and the Ig1-2 Jurkat clone with similar efficiency, suggesting that the presence of a membrane-distal epitope is not necessarily inhibitory if the same epitope is also located proximally (Fig. 6*A*). Next, we tested whether efficient signaling could be inhibited by the presence of a large extracellular domain above a membrane-proximal epitope. This might sterically limit Ag recognition and possibly impede close effector:target membrane apposition by preventing the clearance of a large extracellular domain protein from the target:effector contact site, normally comprised by small extracellular domain proteins (21). We therefore generated a rearranged ligand, denoted Ig3-7;1-2, that contained the third through seventh Ig-like domains of CD22, followed by the first two Ig-like domains now placed proximal to the membrane, and the full transmembrane and intracellular sequences of CD22 (Fig. 6*B*). Jurkat T cells were transduced with this ligand and sorted for high expression of the RFB4 epitope equivalent to cells selected for high expression of WT CD22. Lysis of this cell line by the CD22-specific CTL was then analyzed. The RFB4 cTCR$^+$ CTL line lysed the Ig3-7;1-2$^+$ cell line half as efficiently as the WT CD22$^+$ Jurkat cell line, consistent with the increased distance of the third Ig domain from the membrane (Fig. 6*C*). In contrast, the HD39 cTCR$^+$ CTL lysed the Ig3-7;1-2$^+$ cell line as efficiently as the Ig1-2$^+$ cell line, suggesting that large extracellular domains above a membrane-proximal epitope are not inhibitory to efficient signaling. Our data suggest that membrane-distal epitopes or large extracellular domains above target ligand epitopes are not intrinsically inhibitory to efficient cTCR signaling provided that a membrane-proximal ligand is present. Therefore, targeting a membrane-proximal epitope on a tumor cell would not necessarily be impeded by the presence of a larger isoform on the same cell containing the epitope in a membrane-distal position.

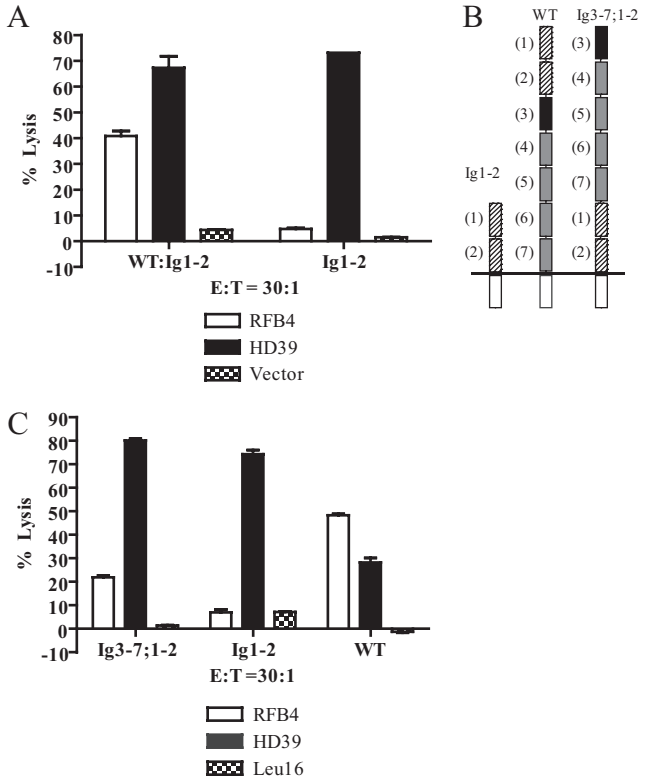

FIGURE 6. Membrane-distal target epitopes are not inhibitory in the presence of membrane-proximal ones. *A*, Lysis of CD22 WT^{high} $Ig1\text{-}2^{high}$ or $Ig1\text{-}2^{high}$ Jurkat cell lines by RFB4, HD39, or empty vector-transduced CTL. Lysis was analyzed by the 7-AAD lysis assay. *B*, Schematic of WT CD22, Ig1-2, and rearranged Ig3-7;1-2 CD22-based ligand. *C*, Target lysis of Jurkat cell lines expressing equivalent densities of WT CD22, Ig1-2, and Ig3-7;1-2 ligands by RFB4, HD39, or Leu16 $cTCR^+$ CTL. Lysis was analyzed by the 7-AAD lysis assay. Data are representative results from one of three experiments. Average and SD of duplicate samples are shown for *A* and *C*.

Diminished lytic sensitivity of CD22-specific cTCR targeting WT CD22 permits selective lysis of tumor cell lines while demonstrating minimal activity against normal, autologous B cells

Previous investigations have demonstrated that CTL expressing low-affinity cTCR (40) or demonstrating low cTCR expression densities (41) can promote selective lysis, discriminating between targets with disparate Ag densities. We hypothesized that the decreased Ag sensitivity of the CD22-specific cTCR responding to the membrane-distal epitopes in WT CD22 might permit selective lysis of tumor cells and not normal B cells, which express fewer CD22 than CD20 molecules (14, 15). We therefore tested the three $cTCR^+$ CTL lines for lytic activity against the $CD20^+CD22^+$ tumor cell lines Raji and Ramos and against autologous B cells selected for CD19 expression by immunomagnetic sorting. Although the CD20-specific line lysed both tumor lines and autologous B cells efficiently, the CD22-specific lines demonstrated minimal cytotoxicity against autologous B cells (Fig. 7*A*). The RFB4 $cTCR^+$ line demonstrated intermediate lytic activity and lysed the Raji, Ramos, and Daudi tumor cell lines (~30, ~40, and ~60%, respectively; Figs. 7*A* and 1*D*), but mediated nearly undetectable lysis of autologous B cells (Fig. 7*A*). In contrast, the HD39 $cTCR^+$ CTL line demonstrated minimal cytotoxicity toward autologous B cells and relatively low cytotoxicity against the Raji, Ramos, and Daudi tumor cell lines (~10, ~15, and ~40%, respectively; Figs. 7*A* and 1*D*).

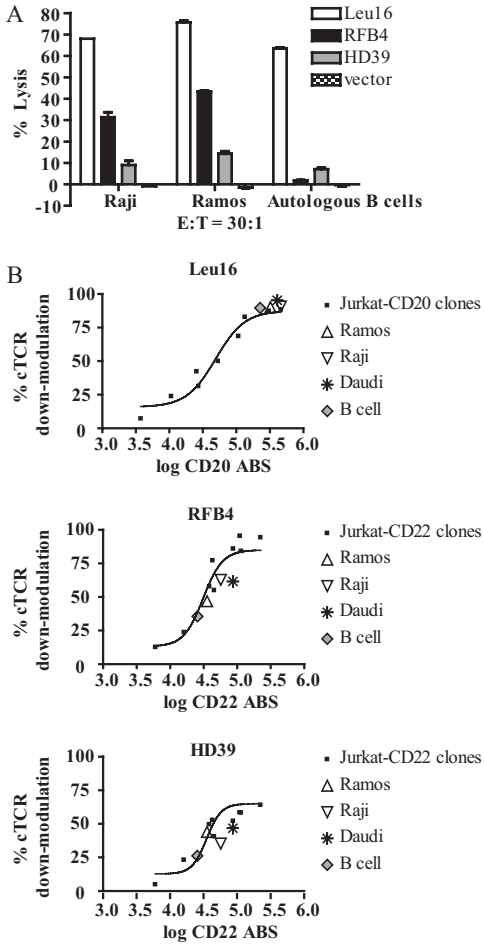

FIGURE 7. Diminished lytic sensitivity of CD22-specific cTCR-targeting WT CD22 permits selective lysis of tumor cell lines and weak responses to normal, autologous B cells. *A*, Target lysis of the B cell lymphoma lines Raji or Ramos and of CD19 positively selected autologous B cells by Leu16, RFB4, and HD39 $cTCR^+$ CTL or empty vector-transduced CTL was assessed by the 7-AAD assay. Average and SD of triplicate samples shown and are representative of four experiments. *B*, cTCR down-modulation in response to tumor cell lines or autologous B cells was assessed by the cTCR down-modulation assay. For comparison, the cTCR down-modulation dose-response curve generated by $cTCR^+$ CTL responding to Jurkat clones expressing varying CD20 or CD22 expression densities is superimposed. Data are representative of two experiments.

To further examine the basis for this differential lysis by the RFB4 cTCR, we investigated cTCR down-modulation in response to tumor cell lines and autologous B cells as a function of target Ag density, as a measure of activation, and compared those values to dose-response curves for cTCR down-modulation generated using CD20- and CD22-transduced Jurkat clones. Normal autologous B cells expressed amounts of CD20 and CD22 very similar to those reported by others: 200,000 CD20 and 25,000 CD22 molecules/cell, respectively (Fig. 7*B*) (14, 15). Both tumor cell lines and autologous B cells maximally induced down-modulation of the Leu16 cTCR, presumably by virtue of the high expression of CD20 (normal B cells, ~200,000; Daudi, ~400,000; Raji, ~380,000; and Ramos, ~300,000 CD20 molecules/cell; average of two experiments; Fig. 7*B*). In contrast, autologous B cells, which express CD22 at a lower density, only modestly induced down-modulation of the CD22-specific cTCR (~35% RFB4, ~25% HD39 cTCR down-modulation). Tumor cell lines induced down-modulation of the CD22-specific cTCR to intermediate values (~45–60% RFB4, ~35–45% HD39), consistent with the

greater lytic activity exhibited by the CD22-specific cTCR in response to lymphoma cells compared with autologous B cells and with the relatively higher CD22 expression on tumor cell lines (Daudi, ~85,000; Raji, ~80,000; Ramos, ~40,000 molecules/cell; average of two experiments; Fig. 7*B*). These data suggest that the RFB4 cTCR may allow selective lysis of $CD22^{high}$ tumor cells in lymphoma patients without lysing normal B cells to a significant extent, and furthermore, might improve T cell persistence and function by limiting undesired interactions between $cTCR^+$ CTL and normal B cells, which might lead to anergy or deletion.

Discussion

We have investigated for the first time the potential utility of the CD22 surface molecule as a therapeutic target for the treatment of malignant B cell neoplasms, and have identified insights into Ag recognition by $cTCR^+$ CTL that will most likely aid the design of future cTCR constructs. CD22 can be targeted as a tumor-associated Ag expressed by malignant B cell neoplasms, allowing efficient lysis of $CD22^{high}$ targets by CD22-specific $cTCR^+$ CTL, but these T cells show diminished Ag sensitivity relative to CD20-specific $cTCR^+$ CTL as a result of targeting membrane-distal epitopes of CD22. However, due to this diminished Ag sensitivity, CD22-specific $cTCR^+$ CTL preferentially lyse tumor cell lines overexpressing CD22, while reacting weakly to normal B cells.

We noted that as the size of the cTCR:ligand pair increased, the efficiency of target lysis decreased (Figs. 1*D*, 2*B*, and 7*A*). This is consistent with studies examining primary T cells and T cell hybridomas responding to pMHC ligands of varying size (20), in which ligands exceeding the native TCR:pMHC dimensions severely diminished signaling in primary T cells. Recently, a similar correlation was shown between cTCR:ligand pair size and signaling efficiency with cTCR targeting membrane-proximal or -distal epitopes of carcinoembryonic Ag (22). However, the diminution in lytic potential was less pronounced in that system than in ours, suggesting that differential flexibility of target molecule extracellular domains may modulate this phenomenon. We have extended those previous findings with mechanistic studies demonstrating that targeting membrane-distal epitopes diminishes the strength of the signal delivered per cTCR and produces a granule-targeting defect without affecting the avidity of Ag recognition leading to cTCR engagement and down-modulation. Taken together, these data indicate that both canonical TCR and cTCR are subject to ligand size-based signal attenuation, and suggest that a similar mechanism may be responsible for this phenomenon.

The kinetic segregation model suggests that increased TCR:ligand pair size allows the large extracellular domain-containing phosphatases CD45 and CD148 to gain access to TCR microclusters during Ag recognition, dephosphorylating the TCR and preventing efficient signal transduction to occur (21). An implicit consequence of this model is that a greater number of TCR must be triggered to generate a given quantity of phosphorylated TCR and signal strength when targeting membrane-distal epitopes as compared with membrane-proximal ones. Far fewer Leu16 CD20-specific cTCR needed to be triggered and down-modulated than RFB4 CD22-specific cTCR to promote maximum degranulation or target lysis (Fig. 4), which is consistent with the higher Ag sensitivity of the CD20-specific cTCR (Fig. 2, *B.1* vs *B.2*). Because both of these cTCR recognize Ag and are down-modulated with similar avidity following Ag engagement (Fig. 2, *B* and *D*), the RFB4 cTCR must deliver a weaker signal per triggered cTCR. Targeting membrane-distal epitopes therefore might generate signals similar to partial agonists (which are characterized by partial CD3ζ phosphorylation (31, 36, 42)), consistent with evidence that recognition of artificially elongated pMHC molecules produces deficient CD3ζ phosphorylation (20) and that diminished signaling is observed with ligands that poorly phosphorylate CD3ζ (31, 42). The HD39 cTCR demonstrated EC_{50} values for lysis and degranulation nearly identical with those observed for the RFB4 cTCR (Figs. 2*B* and 3), suggesting the HD39 cTCR also promotes a weaker signal than the Leu16 cTCR. Because the HD39 cTCR can promote efficient lysis and degranulation in response to cells expressing the same epitope located more proximal to the membrane (Fig. 5, *C–E*), the observed signaling defects do not reflect insufficient cTCR expression density nor intrinsic signaling defects of this particular cTCR. Instead, the data imply that cTCR signaling strength, and as a result Ag sensitivity, is decreased as the target epitope distance from the target cell membrane increases.

Based on the kinetic segregation model, we hypothesized that membrane-distal epitopes might inhibit efficient signaling in the presence of membrane-proximal ones by competing for cTCR binding and by generating an enlarged effector:target intermembrane distance, permitting phosphatases to enter the formed microcluster and dephosphorylate activated molecules of the signaling cascade, similar to mechanisms proposed for antagonistic pMHC molecules (43–47). Moreover, membrane-distal epitopes might actually be preferentially engaged compared with proximal ones, because these epitopes may be more accessible. In contrast, we found that the HD39 cTCR promoted equivalent lysis of target cells expressing a truncated CD22-based ligand in the presence or absence of WT CD22 containing the epitope distal to the membrane (Fig. 6*A*), suggesting efficient cTCR recognition of the truncated ligand. We also found that the HD39 cTCR could promote equivalent lysis of targets expressing either the truncated Ig1-2 CD22 molecule or a rearranged CD22 molecule containing a membrane-proximal epitope with a large extracellular domain above it (Fig. 6*C*). This suggests that lack of exclusion of a protein with a large extracellular domain from effector:target contact points does not necessarily inhibit efficient signaling. Our results thus demonstrate that cTCR can produce efficient signaling if a membrane-proximal ligand is present, regardless of the presence of membrane-distal ones.

Our results could be consistent with the kinetic segregation model if cTCR could preferentially engage membrane-proximal ligands and exclude ligands with distal epitopes from regions of tight membrane apposition generated by this preferential engagement, similar to exclusion of molecules such as CD45 and CD148 during $\alpha\beta$ TCR-mediated Ag recognition (37, 48). This process might be thermodynamically favored by allowing coaptation of the smaller, topologically equivalent adhesion molecule CD2 with CD58 (in humans) or with CD48 (in mice). A similar phenomenon has been observed with enhanced CD28:B7 interactions occurring in the presence of interactions of the equivalently sized CD2:CD48 molecules, but not the larger LFA-1:ICAM-1 molecules (49). This suggests that a similar topological sorting might be possible for cTCR targeting differentially sized ligands. Even in the absence of CD2:CD58 or CD2:CD48 interactions, the high affinity of scFv cTCR may be sufficient to rivet the target and effector cell membranes together such that large cTCR:ligand pairs and phosphatases with large extracellular domains are excluded, generating a microenvironment conducive to phosphorylation and efficient signal transduction.

Our investigation of the effect of cTCR:ligand pair size on the Ag sensitivity and efficiency of degranulation and target lysis revealed that the RFB4 and the HD39 CD22-specific cTCR demonstrate a granule-targeting defect when engaged by WT CD22. Although both the Leu16 and RFB4 cTCR mediate maximal degranulation at saturating Ag densities (Fig. 3), the maximum lysis induced by this degranulation by the Leu16 CD20-specific

cTCR at saturating Ag density is almost twice that achieved by the RFB4 CD22-specific cTCR. A similar lytic granule-targeting defect has recently been described from blockade with mAb of LFA-1:ICAM-1 interactions (50), which had no effect on degranulation, but rather interfered with granule polarization, resulting in a ~50% reduction in lysis. More recently, confocal microscopy revealed that blockade of LFA-1:ICAM-1 interactions prevented exclusion of CD45 from regions of TCR signaling (51), as reported with canonical TCR chains targeting epitopes engineered to be more membrane distal than a classical pMHC complex (20). These results suggest that targeting membrane-distal epitopes with cTCR may preclude proper LFA-1:ICAM-1 interactions, resulting in a defect in granule polarization and targeting. Such lack of adhesive interactions may also inhibit tight apposition of CTL and target membranes, which normally occurs during target lysis by CTL (52). These data suggest that strategies to modify cTCR to enhance signal strength may still fail to completely overcome the diminished target lysis observed when $cTCR^+$ CTL target membrane-distal epitopes.

Analysis of cTCR Ag sensitivity suggests that even when targeting ligands of optimal size, cTCR require very large numbers of Ag molecules (~10^4 ligands) to achieve half-maximal lysis values (Figs. 2*B.1* and 5*E*) compared with $\alpha\beta$ TCR, which can require fewer than 10 agonistic pMHC/cell (53, 54). Our data suggest that, unlike $\alpha\beta$ TCR, cTCR do not serially engage Ag molecules, most likely due to the high affinity and low dissociation rates of scFv compared with $\alpha\beta$ TCR (Fig. 2*D*). Serial engagement and triggering of $\alpha\beta$ TCR by pMHC have been hypothesized to amplify signal strength in the presence of few pMHC ligands (32, 36), and consequently, loss of serial triggering should diminish the sensitivity of responses such as lysis to target Ag expression. Because serial triggering may reflect activation of ~200 TCR per a single pMHC (36), loss of serial engagement could theoretically result in a decrease in Ag sensitivity of two orders of magnitude. Previous work has suggested that loss of serial engagement resulting from long TCR:pMHC association times can lower Ag sensitivity (55, 56). These results suggest that the high affinity of our cTCR may limit their Ag sensitivity by abrogating serial triggering.

Finally, we have defined conditions under which CTL can be genetically modified to express cTCR recognizing CD22 and selectively target malignant B cells for lysis, while reacting weakly to normal B cells. The RFB4 cTCR, which binds an epitope at an intermediate distance from the target cell membrane relative to the Leu16 and HD39 cTCR, promoted relatively efficient lysis of tumor cell lines while not lysing autologous B cells to a great extent (Figs. 1*D* and 7*A*). The failure of cells expressing the RFB4 cTCR to respond strongly to normal B cells may mitigate induction of anergy or deletion of CTL expressing this receptor, allowing enhanced antitumor activity in lymphoma patients with high numbers of circulating normal B cells. Our data suggest that differential choice of epitopes may allow modulation of Ag sensitivity, and that, as shown previously, a greater degree of discrimination between targets of disparate Ag density can be achieved by cTCR with lower sensitivity (40). The adhesion molecules neural cell adhesion molecule, L1 cell adhesion molecule, E-selectin, VCAM-1, and N-cadherin and some cell surface receptors such as platelet-derived growth factor receptor α contain large extracellular domains and are overexpressed in many cancers originating in the lung, CNS, prostate, breast, ovary, kidney, colon, and other tissues (57–63). Therefore, targeting membrane-distal epitopes of overexpressed adhesion molecules or other large extracellular domain-containing molecules with cTCR might represent a novel strategy to modulate cTCR sensitivity and promote selective lysis of tumors, while sparing healthy tissue.

Although this approach takes advantage of Ags that are expressed at higher levels in tumors compared with normal cells, we recognize that by lowering the Ag sensitivity and maximum lytic potential of $cTCR^+$ CTL, the outgrowth of tumors expressing lower target Ag densities (i.e., similar to normal cells) might be promoted. In vivo studies will need to be performed to determine whether attenuating reactivity to self Ags abundant on tumor cells will provide sufficient advantage to a $cTCR^+$ CTL to permit tumor eradication while circumventing deletion or anergy induced by Ag-expressing normal tissues, and therefore justify the diminished Ag sensitivity resulting from targeting membrane-distal epitopes on tumors. In conclusion, our results suggest that targeting surface Ags with engineered cTCR is subject to basic constraints imposed by the underlying biology of T cells, and that a greater understanding of these factors may allow design of receptors that exploit the properties of cTCR to achieve selective and efficient lysis of malignant cells with relative preservation of healthy tissue. We are optimistic that such reagents may eventually improve the management of patients with recurrent B cell neoplasms and other malignancies.

Acknowledgments

We thank Nural Orgun and Dr. Ryan Teague for a critical review of the manuscript.

Disclosures

The authors have no financial conflict of interest.

References

1. Wang, J., O. W. Press, C. G. Lindgren, P. Greenberg, S. Riddell, X. Qian, C. Laugen, A. Raubitschek, S. J. Forman, and M. C. Jensen. 2004. Cellular immunotherapy for follicular lymphoma using genetically modified CD20-specific $CD8^+$ cytotoxic T lymphocytes. *Mol. Ther.* 9: 577–586.
2. Jensen, M. C., P. Clarke, G. Tan, C. Wright, W. Chung-Chang, T. N. Clark, F. Zhang, M. L. Slovak, A. M. Wu, S. J. Forman, and A. Raubitschek. 2000. Human T lymphocyte genetic modification with naked DNA. *Mol. Ther.* 1: 49–55.
3. Jensen, M., G. Tan, S. Forman, A. M. Wu, and A. Raubitschek. 1998. CD20 is a molecular target for scFvFc:ζ receptor redirected T cells: implications for cellular immunotherapy of $CD20^+$ malignancy. *Biol. Blood Marrow Transplant.* 4: 75–83.
4. Stashenko, P., L. M. Nadler, R. Hardy, and S. F. Schlossman. 1980. Characterization of a human B lymphocyte-specific antigen. *J. Immunol.* 125: 1678–1685.
5. Anderson, K. C., M. P. Bates, B. L. Slaughenhoupt, G. S. Pinkus, S. F. Schlossman, and L. M. Nadler. 1984. Expression of human B cell-associated antigens on leukemias and lymphomas: a model of human B cell differentiation. *Blood* 63: 1424–1433.
6. Maloney, D. G., A. J. Grillo-Lopez, D. J. Bodkin, C. A. White, T. M. Liles, I. Royston, C. Varns, J. Rosenberg, and R. Levy. 1997. IDEC-C2B8: results of a phase I multiple-dose trial in patients with relapsed non-Hodgkin's lymphoma. *J. Clin. Oncol.* 15: 3266–3274.
7. McLaughlin, P. 2001. Rituximab: perspective on single agent experience, and future directions in combination trials. *Crit. Rev. Oncol. Hematol.* 40: 3–16.
8. McLaughlin, P., A. J. Grillo-Lopez, B. K. Link, R. Levy, M. S. Czuczman, M. E. Williams, M. R. Heyman, I. Bence-Bruckler, C. A. White, F. Cabanillas, et al. 1998. Rituximab chimeric anti-CD20 monoclonal antibody therapy for relapsed indolent lymphoma: half of patients respond to a four-dose treatment program. *J. Clin. Oncol.* 16: 2825–2833.
9. Press, O. W., F. Appelbaum, J. A. Ledbetter, P. J. Martin, J. Zarling, P. Kidd, and E. D. Thomas. 1987. Monoclonal antibody 1F5 (anti-CD20) serotherapy of human B cell lymphomas. *Blood* 69: 584–591.
10. Press, O. W., J. F. Eary, F. R. Appelbaum, P. J. Martin, C. C. Badger, W. B. Nelp, S. Glenn, G. Butchko, D. Fisher, B. Porter, et al. 1993. Radiolabeled-antibody therapy of B-cell lymphoma with autologous bone marrow support. *N. Engl. J. Med.* 329: 1219–1224.
11. Gaipa, G., G. Basso, O. Maglia, V. Leoni, A. Faini, G. Cazzaniga, C. Bugarin, M. Veltroni, B. Michelotto, R. Ratei, T. Coliva, et al. 2005. Drug-induced immunophenotypic modulation in childhood ALL: implications for minimal residual disease detection. *Leukemia* 19: 49–56.
12. Rocha, B., A. Grandien, and A. A. Freitas. 1995. Anergy and exhaustion are independent mechanisms of peripheral T cell tolerance. *J. Exp. Med.* 181: 993–1003.
13. Vitetta, E. S., M. Stone, P. Amlot, J. Fay, R. May, M. Till, J. Newman, P. Clark, R. Collins, D. Cunningham, et al. 1991. Phase I immunotoxin trial in patients with B-cell lymphoma. *Cancer Res.* 51: 4052–4058.
14. Rossmann, E. D., J. Lundin, R. Lenkei, H. Mellstedt, and A. Osterborg. 2001. Variability in B-cell antigen expression: implications for the treatment of B-cell lymphomas and leukemias with monoclonal antibodies. *Hematol. J.* 2: 300–306.

15. Wang, L., F. Abbasi, A. K. Gaigalas, R. F. Vogt, and G. E. Marti. 2006. Comparison of fluorescein and phycoerythrin conjugates for quantifying CD20 expression on normal and leukemic B-cells. *Cytometry B Clin. Cytom.* 70: 410–415.
16. Polyak, M. J., S. H. Tailor, and J. P. Deans. 1998. Identification of a cytoplasmic region of CD20 required for its redistribution to a detergent-insoluble membrane compartment. *J. Immunol.* 161: 3242–3248.
17. Einfeld, D. A., J. P. Brown, M. A. Valentine, E. A. Clark, and J. A. Ledbetter. 1988. Molecular cloning of the human B cell CD20 receptor predicts a hydrophobic protein with multiple transmembrane domains. *EMBO J.* 7: 711–717.
18. Engel, P., N. Wagner, A. S. Miller, and T. F. Tedder. 1995. Identification of the ligand-binding domains of CD22, a member of the immunoglobulin superfamily that uniquely binds a sialic acid-dependent ligand. *J. Exp. Med.* 181: 1581–1586.
19. Nitschke, L., and T. Tsubata. 2004. Molecular interactions regulate BCR signal inhibition by CD22 and CD72. *Trends Immunol.* 25: 543–550.
20. Choudhuri, K., D. Wiseman, M. H. Brown, K. Gould, and P. A. van der Merwe. 2005. T-cell receptor triggering is critically dependent on the dimensions of its peptide-MHC ligand. *Nature* 436: 578–582.
21. Davis, S. J., and P. A. van der Merwe. 2006. The kinetic-segregation model: TCR triggering and beyond. *Nat. Immunol.* 7: 803–809.
22. Hombach, A. A., V. Schildgen, C. Heuser, R. Finnern, D. E. Gilham, and H. Abken. 2007. T cell activation by antibody-like immunoreceptors: the position of the binding epitope within the target molecule determines the efficiency of activation of redirected T cells. *J. Immunol.* 178: 4650–4657.
23. Coloma, M. J., J. W. Larrick, M. Ayala, and J. V. Gavilondo-Cowley. 1991. Primer design for the cloning of immunoglobulin heavy-chain leader-variable regions from mouse hybridoma cells using the PCR. *BioTechniques* 11: 152–156.
24. Coloma, M. J., A. Hastings, L. A. Wims, and S. L. Morrison. 1992. Novel vectors for the expression of antibody molecules using variable regions generated by polymerase chain reaction. *J. Immunol. Methods* 152: 89–104.
25. Cooper, L. J., M. S. Topp, C. Pinzon, I. Plavec, M. C. Jensen, S. R. Riddell, and P. D. Greenberg. 2004. Enhanced transgene expression in quiescent and activated human $CD8^+$ T cells. *Hum. Gene Ther.* 15: 648–658.
26. Riddell, S. R., and P. D. Greenberg. 1990. The use of anti-CD3 and anti-CD28 monoclonal antibodies to clone and expand human antigen-specific T cells. *J. Immunol. Methods* 128: 189–201.
27. Takayama, H., G. Trenn, and M. V. Sitkovsky. 1987. A novel cytotoxic T lymphocyte activation assay: optimized conditions for antigen receptor triggered granule enzyme secretion. *J. Immunol. Methods* 104: 183–190.
28. Stein, R., E. Belisle, H. J. Hansen, and D. M. Goldenberg. 1993. Epitope specificity of the anti-(B cell lymphoma) monoclonal antibody, LL2. *Cancer Immunol. Immunother.* 37: 293–298.
29. Schodin, B. A., T. J. Tsomides, and D. M. Kranz. 1996. Correlation between the number of T cell receptors required for T cell activation and TCR-ligand affinity. *Immunity* 5: 137–146.
30. Sykulev, Y., R. J. Cohen, and H. N. Eisen. 1995. The law of mass action governs antigen-stimulated cytolytic activity of $CD8^+$ cytotoxic T lymphocytes. *Proc. Natl. Acad. Sci. USA* 92: 11990–11992.
31. Hemmer, B., I. Stefanova, M. Vergelli, R. N. Germain, and R. Martin. 1998. Relationships among TCR ligand potency, thresholds for effector function elicitation, and the quality of early signaling events in human T cells. *J. Immunol.* 160: 5807–5814.
32. Viola, A., and A. Lanzavecchia. 1996. T cell activation determined by T cell receptor number and tunable thresholds. *Science* 273: 104–106.
33. San Jose, E., A. Borroto, F. Niedergang, A. Alcover, and B. Alarcon. 2000. Triggering the TCR complex causes the down-regulation of nonengaged receptors by a signal transduction-dependent mechanism. *Immunity* 12: 161–170.
34. Annenkov, A. E., G. M. Daly, T. Brocker, and Y. Chernajovsky. 2003. Clustering of immunoreceptor tyrosine-based activation motif-containing signalling subunits in $CD4^+$ T cells is an optimal signal for IFN-γ production, but not for the production of IL-4. *Int. Immunol.* 15: 665–677.
35. Faroudi, M., C. Utzny, M. Salio, V. Cerundolo, M. Guiraud, S. Muller, and S. Valitutti. 2003. Lytic versus stimulatory synapse in cytotoxic T lymphocyte/target cell interaction: manifestation of a dual activation threshold. *Proc. Natl. Acad. Sci. USA* 100: 14145–14150.
36. Valitutti, S., S. Muller, M. Cella, E. Padovan, and A. Lanzavecchia. 1995. Serial triggering of many T-cell receptors by a few peptide-MHC complexes. *Nature* 375: 148–151.
37. Lin, J., and A. Weiss. 2003. The tyrosine phosphatase CD148 is excluded from the immunologic synapse and down-regulates prolonged T cell signaling. *J. Cell Biol.* 162: 673–682.
38. Wild, M. K., A. Cambiaggi, M. H. Brown, E. A. Davies, H. Ohno, T. Saito, and P. A. van der Merwe. 1999. Dependence of T cell antigen recognition on the dimensions of an accessory receptor-ligand complex. *J. Exp. Med.* 190: 31–41.
39. Tedder, T. F., J. Tuscano, S. Sato, and J. H. Kehrl. 1997. CD22, a B lymphocyte-specific adhesion molecule that regulates antigen receptor signaling. *Annu. Rev. Immunol.* 15: 481–504.
40. Chmielewski, M., A. Hombach, C. Heuser, G. P. Adams, and H. Abken. 2004. T cell activation by antibody-like immunoreceptors: increase in affinity of the single-chain fragment domain above threshold does not increase T cell activation against antigen-positive target cells but decreases selectivity. *J. Immunol.* 173: 7647–7653.
41. Weijtens, M. E., E. H. Hart, and R. L. Bolhuis. 2000. Functional balance between T cell chimeric receptor density and tumor associated antigen density: CTL mediated cytolysis and lymphokine production. *Gene Ther.* 7: 35–42.
42. Itoh, Y., B. Hemmer, R. Martin, and R. N. Germain. 1999. Serial TCR engagement and down-modulation by peptide:MHC molecule ligands: relationship to the quality of individual TCR signaling events. *J. Immunol.* 162: 2073–2080.
43. Daniels, M. A., S. L. Schober, K. A. Hogquist, and S. C. Jameson. 1999. Cutting edge: a test of the dominant negative signal model for TCR antagonism. *J. Immunol.* 162: 3761–3764.
44. Stefanova, I., B. Hemmer, M. Vergelli, R. Martin, W. E. Biddison, and R. N. Germain. 2003. TCR ligand discrimination is enforced by competing ERK positive and SHP-1 negative feedback pathways. *Nat. Immunol.* 4: 248–254.
45. Dittel, B. N., I. Stefanova, R. N. Germain, and C. A. Janeway, Jr. 1999. Cross-antagonism of a T cell clone expressing two distinct T cell receptors. *Immunity* 11: 289–298.
46. Robertson, J. M., and B. D. Evavold. 1999. Cutting edge: dueling TCRs: peptide antagonism of $CD4^+$ T cells with dual antigen specificities. *J. Immunol.* 163: 1750–1754.
47. Stotz, S. H., L. Bolliger, F. R. Carbone, and E. Palmer. 1999. T cell receptor (TCR) antagonism without a negative signal: evidence from T cell hybridomas expressing two independent TCRs. *J. Exp. Med.* 189: 253–264.
48. Varma, R., G. Campi, T. Yokosuka, T. Saito, and M. L. Dustin. 2006. T cell receptor-proximal signals are sustained in peripheral microclusters and terminated in the central supramolecular activation cluster. *Immunity* 25: 117–127.
49. Bromley, S. K., A. Iaboni, S. J. Davis, A. Whitty, J. M. Green, A. S. Shaw, A. Weiss, and M. L. Dustin. 2001. The immunological synapse and CD28–CD80 interactions. *Nat. Immunol.* 2: 1159–1166.
50. Anikeeva, N., K. Somersalo, T. N. Sims, V. K. Thomas, M. L. Dustin, and Y. Sykulev. 2005. Distinct role of lymphocyte function-associated antigen-1 in mediating effective cytolytic activity by cytotoxic T lymphocytes. *Proc. Natl. Acad. Sci. USA* 102: 6437–6442.
51. Graf, B., T. Bushnell, and J. Miller. 2007. LFA-1-mediated T cell costimulation through increased localization of TCR/class II complexes to the central supramolecular activation cluster and exclusion of CD45 from the immunological synapse. *J. Immunol.* 179: 1616–1624.
52. Stinchcombe, J. C., G. Bossi, S. Booth, and G. M. Griffiths. 2001. The immunological synapse of CTL contains a secretory domain and membrane bridges. *Immunity* 15: 751–761.
53. Purbhoo, M. A., D. J. Irvine, J. B. Huppa, and M. M. Davis. 2004. T cell killing does not require the formation of a stable mature immunological synapse. *Nat. Immunol.* 5: 524–530.
54. Kageyama, S., T. J. Tsomides, Y. Sykulev, and H. N. Eisen. 1995. Variations in the number of peptide-MHC class I complexes required to activate cytotoxic T cell responses. *J. Immunol.* 154: 567–576.
55. Gonzalez, P. A., L. J. Carreno, D. Coombs, J. E. Mora, E. Palmieri, B. Goldstein, S. G. Nathenson, and A. M. Kalergis. 2005. T cell receptor binding kinetics required for T cell activation depend on the density of cognate ligand on the antigen-presenting cell. *Proc. Natl. Acad. Sci. USA* 102: 4824–4829.
56. Kalergis, A. M., N. Boucheron, M. A. Doucey, E. Palmieri, E. C. Goyarts, Z. Vegh, I. F. Luescher, and S. G. Nathenson. 2001. Efficient T cell activation requires an optimal dwell-time of interaction between the TCR and the pMHC complex. *Nat. Immunol.* 2: 229–234.
57. Gavert, N., M. Conacci-Sorrell, D. Gast, A. Schneider, P. Altevogt, T. Brabletz, and A. Ben-Ze'ev. 2005. L1, a novel target of β-catenin signaling, transforms cells and is expressed at the invasive front of colon cancers. *J. Cell Biol.* 168: 633–642.
58. Gavert, N., M. Sheffer, S. Raveh, S. Spaderna, M. Shtutman, T. Brabletz, F. Barany, P. Paty, D. Notterman, E. Domany, and A. Ben-Ze'ev. 2007. Expression of L1-CAM and ADAM10 in human colon cancer cells induces metastasis. *Cancer Res.* 67: 7703–7712.
59. Bhaskar, V., D. A. Law, E. Ibsen, D. Breinberg, K. M. Cass, R. B. DuBridge, F. Evangelista, S. M. Henshall, P. Hevezi, J. C. Miller, et al. 2003. E-selectin up-regulation allows for targeted drug delivery in prostate cancer. *Cancer Res.* 63: 6387–6394.
60. Matei, D., R. E. Emerson, Y. C. Lai, L. A. Baldridge, J. Rao, C. Yiannoutsos, and D. D. Donner. 2006. Autocrine activation of PDGFRα promotes the progression of ovarian cancer. *Oncogene* 25: 2060–2069.
61. Hulit, J., K. Suyama, S. Chung, R. Keren, G. Agiostratidou, W. Shan, X. Dong, T. M. Williams, M. P. Lisanti, K. Knudsen, and R. B. Hazan. 2007. N-cadherin signaling potentiates mammary tumor metastasis via enhanced extracellular signal-regulated kinase activation. *Cancer Res.* 67: 3106–3116.
62. Jensen, M., and F. Berthold. 2007. Targeting the neural cell adhesion molecule in cancer. *Cancer Lett.* 258: 9–21.
63. Wu, T. C. 2007. The role of vascular cell adhesion molecule-1 in tumor immune evasion. *Cancer Res.* 67: 6003–6006.